

Non-Equilibrium Quantum Interference in Metallic Mesoscopic Systems

C. Terrier, D. Babić, C. Strunk, T. Nussbaumer and C. Schönenberger

Institute of Physics, University of Basel, Klingelbergstrasse 82, CH-4056 Basel, Switzerland

We study the influence of a DC bias voltage V on quantum interference corrections to the measured differential conduction in mesoscopic wires and rings. The amplitude of both universal conductance fluctuations (UCF) and Aharonov-Bohm effect (ABE) is enhanced by several 100 % for voltages larger than the Thouless energy. The enhancement persists even in the presence of inelastic electron-electron scattering up to $V \sim 1$ mV. For larger voltages electron-phonon collisions lead to the amplitude decaying as a power law for the UCF and exponentially for the ABE. A quantitative description is obtained.

PACS: 73.23.-b, 72.10.-d

If size of a conductor is of order of the electron phase-coherence length $L_\varphi(T)$ the wave character of electrons leads to experimentally observable quantum interference contributions to the conductance G . These are the aperiodic and periodic fluctuations δG of the conductance around its average value. In the former case, called universal conductance fluctuations, the interference pattern is formed as a superposition of contributions from a continuous range of possible interference paths. Averaged over either impurity configuration, magnetic field or the Fermi energy, the root-mean-square (rms) conductance fluctuation δG_{rms} is of the order $\sim e^2/h$ [1]. The periodic fluctuations, known as the Aharonov-Bohm effect [2], are observed if the interference is imposed by geometry of a sample, most commonly in the form of a loop. If the loop is threaded by a magnetic flux ϕ , $\delta G(\phi)$ exhibits periodic oscillations with a period h/e , and δG_{rms} is again $\sim e^2/h$. The above behaviour is characteristic of equilibrium conditions, i.e. of $eV \ll k_B T, E_c$, where E_c is the coherence energy (Thouless energy) determined by the size of the conductor. In non-equilibrium ($eV \gg E_c, k_B T$) the fluctuations are expected to be remarkably different, as predicted theoretically by Larkin and Khmel'nitskiĭ (LK) [3]. If inelastic processes can be neglected the rms fluctuation δg_{rms} of the *differential conductance* g increases with V according to $\delta g_{rms} \sim (e^2/h)\sqrt{V/V_c}$, where $V_c = E_c/e$. This, at first sight surprising result, can be understood as follows. At $V \gg V_c$ the relevant energy range for the transport subdivides into $N = V/V_c$ uncorrelated energy intervals, each contributing to the fluctuations of the current by an amount $\sim (e^2/h)V_c$. Incoherent superposition of these contributions leads to δg_{rms} being $N^{1/2}$ times larger than e^2/h . Inelastic scattering at large voltages destroys quantum interference. The enhancement of $\delta g_{rms}(V)$ is thereby suppressed and δg_{rms} eventually decreases with increasing voltage [3]. Experimental studies of both the UCF [4–7] and ABE [4,8,9] under non-equilibrium conditions have been done, but are incomplete. For instance, [6] reported on a voltage-independent δg_{rms} , [4] on a decrease of $\delta g_{rms}(V)$ for $V > V_c$, whereas in [7–9] it was found that $\delta g_{rms}(V)$ shows a non-monotonic behaviour.

In this paper we report on the non-equilibrium UCF

and ABE in diffusive gold samples measured over a wide voltage range of $V \gg k_B T/e, V_c$ that covers both the low-voltage $(V/V_c)^{1/2}$ enhancement of δg_{rms} and its suppression at large voltages. Emphasis is put on the decay of $\delta g_{rms}^{UCF}(V)$ and $\delta g_{rms}^{ABE}(V)$. It is shown that $\delta g_{rms}(V)$ decays as a power law for the UCF and exponentially for the ABE. A quantitative comparison between theory and the experiments allows to extract the voltage-dependent phase-coherence length $L_\varphi(V)$ which we compare with the equilibrium values deduced from the measured weak localisation.

The samples were produced by electron-beam lithography and evaporation of gold. The substrate was silicon covered with 400 nm SiO₂. Three 20 nm thick samples of different planar geometries were prepared: (1) for the ABE measurements a ring of average diameter 1 μm and line width 0.09 μm (sample S_{ABE}); (2) for the UCF measurements a $L_w = 1.5$ μm long and 0.13 μm wide wire (sample S_{UCF}); (3) for the weak-localisation (WL) measurements a 98 μm long and 0.17 μm wide wire (sample S_{WL}). Sample S_{WL} was made relatively long in order to suppress the UCF. All samples were produced under identical conditions (the same source of gold and the same evaporation parameters). The diffusion constants D are consequently very similar: 116 cm²/s for samples S_{UCF} and S_{WL} , and 110 cm²/s for sample S_{ABE} . The measurements were carried out in a ³He cryostat with cryogenic rf-filtering, using a low frequency (37 Hz) lock-in technique to measure the differential conductance. Typical voltage resolution was ~ 0.3 nV. Non-equilibrium UCF and ABE were measured at $T = 300$ mK by superimposing a comparatively large DC bias voltages V_{DC} to the small excitation voltage V_{AC} . The following hierarchy of energies was always maintained: $eV_{DC} \gg k_B T \gtrsim eV_{AC} > E_c$. Ensemble averaging was achieved by measuring the UCF and ABE over a magnetic-field range of ~ 2 T, largely exceeding the correlation field. Typical sweep rates were 0.1 mT/s. Fig.1a displays raw data of a differential-conductance measurement on sample S_{ABE} , taken at $V_{DC} = 0.5$ mV. Both types of the fluctuations are present. In Fig.1b we show the Fourier transform of the same data, exhibiting a well-defined peak at the position corresponding to $\phi = h/e$.

From the magnetoconductance traces we have extracted δg_{rms}^{ABE} and δg_{rms}^{UCF} for sample S_{ABE} , as shown in Fig.2 (discussed in more detail later), and δg_{rms}^{UCF} for sample S_{UCF} .

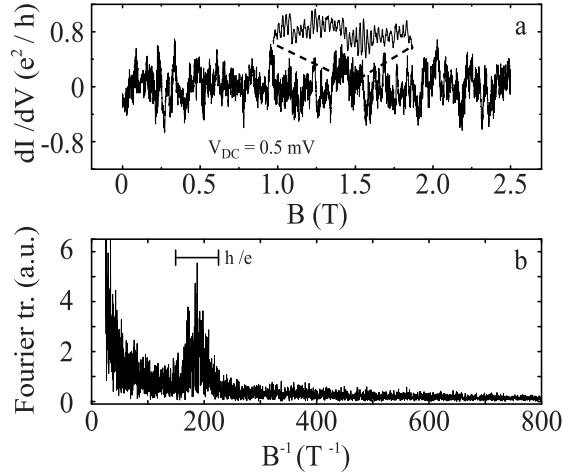


FIG. 1. (a) A differential-magnetoconductance trace of sample S_{ABE} , taken at $V_{DC} = 0.5$ mV. Both the periodic (expanded view) and aperiodic fluctuations are present. (b) Fourier transform of (a), showing a well-defined peak at the position corresponding to $\phi = h/e$.

The WL was measured on sample S_{WL} in equilibrium ($V_{DC} = 0$) and in the temperature range 0.3 - 10 K. By fitting a one-dimensional WL expression [10] to the low-field magnetoconductance data we obtained $L_\varphi(T)$ as a function of temperature, shown in the inset to Fig.3. Similarly to published work [11,12], $L_\varphi(T)$ saturates at low temperatures (below 1 K), whereas at higher temperatures follows two distinct $L_\varphi \propto T^{-q}$ dependences. In a narrow temperature range (1 - 2 K) the exponent q is roughly 1/3, predicted theoretically for dephasing by electron-electron interaction. At higher temperatures q takes a value close to 1.2, suggesting the appearance of electron-phonon interaction. At $T = 300$ mK, $L_\varphi = 3$ μm and $\tau_\varphi = \sqrt{L_\varphi^2/D} = 0.77$ ns, implying that in equilibrium the diffusion of electrons is coherent throughout the samples S_{UCF} and S_{ABE} . L_φ has to be compared further with the effective length of the sample L_{c0} which depends on the particular geometry and the coherence phenomenon investigated. For the UCF in sample S_{UCF} , $L_{c0} = L_w = 1.5$ μm . In the case of ABE in sample S_{ABE} , $L_{c0} = C_r \approx 3.14$ μm , where C_r is the circumference of the ring. Finally, for the UCF in sample S_{ABE} , L_{c0} is calculated as the distances ring - voltage contacts plus $C_r/2$, which gives ≈ 2.2 μm . Thus, $L_\varphi(300\text{ mK}) \gtrsim L_{c0}$, so that the equilibrium coherence energy is set geometrically according to $E_{c0} = eV_{c0} = \hbar D/L_{c0}^2$.

With increasing temperature or applied voltage the coherence length decreases, and once it becomes shorter than L_{c0} the interference contributions are suppressed.

The effect of temperature has been demonstrated by Milliken *et al* [13]. Their method was to determine $L_\varphi(T)$ from the WL and to use this to describe the decay of the *equilibrium* δG , which turned out to be a power law for the UCF and exponential for the ABE. Our approach is complementary: we keep the bath temperature constant and investigate the voltage dependence of the *non-equilibrium* δg . While Milliken *et al.* have observed a monotonically-decreasing $\delta G(T)$, in our case $\delta g(V)$ is a non-monotonic function as shown in Fig.2 for small V_{DC} (but still much larger than V_{c0}), δg_{rms} is enhanced by V_{DC} . At higher voltages δg_{rms} decreases with V_{DC} , *faster in the case of the ABE*, which is in qualitative agreement with the results of Milliken *et al.*

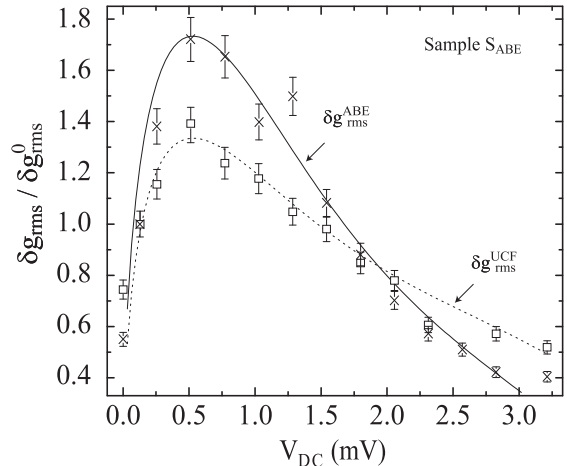


FIG. 2. Plot of δg_{rms}^{ABE} (crosses) and δg_{rms}^{UCF} (open squares) vs. V_{DC} for sample S_{ABE} , with δg_{rms} normalized to the values δg_{rms}^0 at the first $V_{DC} \neq 0$ points (which also satisfy the criterion $V_{DC} \gg V_{c0}$). The lines are plots of Eq.1 (dashed line) and Eq.2 (solid line) deduced in the text.

Let us first turn to the details of non-equilibrium UCF. For convenience we denote the phase-coherence length at a finite bias voltage by $L_\varphi(V)$, while $L_\varphi(T)$ refers to the equilibrium value. If $V_{DC} \gg V_{c0}$, $k_B T/e$ and $L_\varphi(V_{DC}) > L_{c0}$, the LK enhancement of δg_{rms} holds and one expects that $\delta g_{rms} \propto \sqrt{V_{DC}/V_{c0}}$. Once $L_\varphi(V_{DC})$ becomes substantially smaller than L_{c0} inelastic processes start to be important for most of the electrons, and the sample effectively subdivides into L_{c0}/L_φ uncorrelated coherent resistors in series. The LK enhancement in a single ‘resistor’ is still valid if the voltage drop $V_{DC}^{res} = V_{DC}(L_\varphi/L_{c0})$ over a ‘resistor’ exceeds the corresponding coherence voltage $V_c^{res} = V_{c0}(L_{c0}/L_\varphi)^2$. Following the LK arguments, δg_{rms} corresponding to a single ‘resistor’ is proportional to $(V_{DC}^{res}/V_c^{res})^{1/2} = [(V_{DC}/V_{c0})(L_\varphi/L_{c0})^3]^{1/2}$. Incoherent addition of these contributions of ‘resistors’ in series leads to

$$\delta g_{rms}^{UCF} = A_{UCF} \frac{e^2}{h} \sqrt{\frac{V_{DC}}{V_{c0}}} \left(\frac{L_\varphi(V_{DC})}{L_{c0}} \right)^2, \quad (1)$$

where A_{UCF} is a constant. This expression is valid if $V_{DC} > V_{c0}$ and $L_\varphi < L_{c0}$ [14]. It enables the unambiguous determination of $L_\varphi(V_{DC})$. We fix A_{UCF} by ignoring the $(L_\varphi/L_{c0})^2$ term for the first measured point which satisfies $V_{DC} \gg V_{c0}$, and then simply extract $L_\varphi(V_{DC})$ for all the other points from the measured data. For the two sets of UCF data, i.e. for samples S_{UCF} and S_{ABE} , we have obtained excellent agreement in $L_\varphi(V_{DC})$, as we show in Fig.3 by open (S_{ABE}) and full (S_{UCF}) squares. Normalised to the corresponding values of L_{c0} both results collapse onto a single curve. The phase-coherence length deduced from our non-equilibrium experiment $L_\varphi(V)$ has a qualitatively similar dependence as $L_\varphi(T)$ obtained from WL in equilibrium. Two regimes with different power-law dependences are discernible. In the region of increasing $\delta g_{rms}(V_{DC})$ there is a power law $L_\varphi(V_{DC}) \propto V_{DC}^{-s}$, where $s = 0.19 \pm 0.02$. For decreasing $\delta g_{rms}(V_{DC})$, i.e. where $L_\varphi(V_{DC})$ is considerably smaller than L_{c0} , the dependence changes to $L_\varphi \propto V_{DC}^{-p}$ with $p = 0.57 \pm 0.03$. Inserting thus found L_φ back into Eq.1 results in the dotted line in Fig.2. A quantitative comparison between $L_\varphi(V)$ and $L_\varphi(T)$ will be given below.

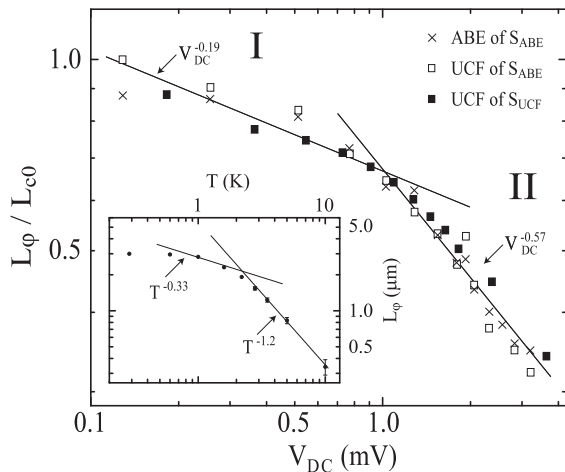


FIG. 3. Phase coherence length $L_\varphi(V_{DC})$, normalised to the characteristic lengths L_{c0} defined in the text, deduced from the non-equilibrium UCF and ABE measurements. Crosses: ABE in sample S_{ABE} . Open squares: UCF in sample S_{ABE} . Full squares: UCF in sample S_{UCF} . Below $V_{DC} \sim 1$ mV, $L_\varphi \propto V_{DC}^{-0.19 \pm 0.02}$, and above $L_\varphi \propto V_{DC}^{-0.57 \pm 0.03}$. Inset: Equilibrium coherence length $L_\varphi(T)$ found from the WL measurements on sample S_{WL} . Note the similarity of the general behaviours of $L_\varphi(V_{DC})$ and $L_\varphi(T)$.

There is no straightforward way to derive an expression for δg_{rms}^{ABE} directly from the LK theory. Subdivision of a ring into resistors makes no sense in this case, as only those electrons which stay coherent over the whole length C_r contribute to the interference. However, since the same physics governs the UCF and ABE, δg_{rms}^{ABE} is expected to be $\propto \sqrt{V_{DC}/V_{c0}}$ in the regime where inelastic scattering is absent. This is indeed the case, as

shown in Fig.2. The form of the suppression of δg_{rms}^{ABE} can be inferred from a theoretical analysis of DiVincenzo and Kane [15]. They have shown that inelastic processes influence the ABE in two ways. First, the fluctuations are suppressed as $\exp(-\beta C_r/L_\varphi)$, where β is of order unity in the range $1 \lesssim C_r/L_\varphi \lesssim 3$ and smaller in the case of a true exponential decay occurring in the asymptotic limit $C_r/L_\varphi \rightarrow \infty$. Second, the proper form of E_c in the presence of inelastic processes is given by $E_c^{in} = \hbar D/C_r^{2-\alpha} L_\varphi^\alpha = E_{c0}(C_r/L_\varphi)^\alpha$ with $\alpha \approx 1.3$. This renormalisation of the coherence energy is a consequence of the statistics for those electrons that diffuse around a ring without being scattered inelastically [15]. Roughly, the probability distribution for an electron to contribute to the ABE has a maximum at a value of the electron traversal time $\sim D/C_r L_\varphi$ [15]. Combining the above arguments we can write for $L_\varphi < C_r$:

$$\delta g_{rms}^{ABE} = A_{ABE} \frac{e^2}{h} \sqrt{\frac{V_{DC}}{V_{c0}}} \left(\frac{L_\varphi(V_{DC})}{C_r} \right)^{0.65} e^{-\beta C_r/L_\varphi(V_{DC})}. \quad (2)$$

Good agreement of the ABE data with Eq.2 and the UCF data is obtained for $\beta \approx 1.1$, as we show in Fig.2 by the solid curve and in Fig.3 by crosses.

So far we have not discussed how electron heating, expected in this highly non-equilibrium situation [16], affects the interference amplitude. Also, we have not yet compared $L_\varphi(V_{DC})$ with the equilibrium $L_\varphi(T)$. We concentrate on these questions in the rest of the paper. From Figs.2,3 we can distinguish two regimes (denoted by I and II in Fig.3): (I) $\delta g_{rms}(V_{DC})$ is an increasing function and $L_\varphi(V_{DC}) \propto V_{DC}^{-0.19}$, and (II), $\delta g_{rms}(V_{DC})$ is a decreasing function and $L_\varphi(V_{DC}) \propto V_{DC}^{-0.57}$. Since the effective electron temperature $T_e(V_{DC})$ is supposed to increase with increasing V_{DC} , $L_\varphi(V_{DC})$ and $L_\varphi(T)$ should display a qualitatively similar dependence, as observed in Fig.3. Below we substantiate this and show that the former behaviour corresponds to electron-electron collisions (out of equilibrium) and the latter to electron-phonon inelastic collisions (in local equilibrium).

The phase-coherence length is determined by the dephasing rate τ_φ^{-1} via $L_\varphi = \sqrt{D\tau_\varphi}$. τ_φ^{-1} can be expressed as an average of the inelastic scattering rate $\tau_{in}^{-1}(E)$ of electrons at energy E over the possible excitations given by the width of the electron distribution function $f(E)$ [12]. Assuming only electron-electron scattering $\tau_{in,ee}^{-1}(E)$ is approximated by $K(E)k_B T$ (equilibrium) or $K(E)E^2/k_B T$ (non-equilibrium). $K(\epsilon) = \kappa_\eta \epsilon^{-\eta}$ is the kernel function of the Coulomb interaction (ϵ is electron energy relative to the Fermi level), where $\eta = 3/2$ in one dimension is relevant here [12]. In equilibrium, where f is the Fermi-Dirac function, one obtains the well-known Nyquist dephasing rate $\tau_{\varphi,ee}^{-1}(T) \propto T^{2/3}$, which results in $L_{\varphi,ee}(T) \propto T^{-1/3}$, indicated in the inset to Fig.3

by a solid line. If for $eV_{DC} \gg k_B T$ the Coulomb interaction would be very strong, f should approach the Fermi-Dirac function, albeit with an elevated electron temperature T_e . If this were the case we would expect $L_{\varphi,ee}(V_{DC}) \propto V_{DC}^{-1/3}$, because $T_e \propto V_{DC}$ in the absence of electron-phonon interactions [17]. This is however not observed, suggesting that the distribution function is a broadened ‘two-step’ function, according to the findings of Pothier *et. al.* [18]. For such a non-equilibrium distribution function $\tau_{\varphi,ee}^{-1}(V) \propto \tau_{in,ee}^{-1}(V) \propto V^{1/2}$ or, equivalently, $L_{\varphi,ee} \propto V^{-1/4}$. This is in fair agreement with our finding $L_{\varphi}(V_{DC}) \propto V_{DC}^{-0.19}$. We emphasise that the rather weak decrease of $L_{\varphi,ee}$ with increasing V is insufficient to suppress the LK enhancement of δg_{rms} . This is seen as follows. We recall that the condition for the appearance of the LK enhancement in a ‘resistor’ is $V_{DC}^{res} > V_c^{res}$, which can be written as $V_{DC}/V_{c0} > (L_{c0}/L_{\varphi})^3$. Since $L_{\varphi,ee} \propto V_{DC}^{-1/4}$, the right-hand side of the above inequality increases more slowly with V_{DC} than the left-hand side, and the condition for the enhancement is maintained over the whole voltage range of increasing $\delta g_{rms}(V_{DC})$.

While the regime I is determined by electron-electron scattering and a non-equilibrium electron distribution function f , the stronger dependence of $L_{\varphi}(V)$ in the regime II is caused by electron-phonon scattering and can be very well described by equilibrium properties taking into account electron heating. Electron-phonon scattering leads to $\tau_{\varphi,ep} \propto T_e^{-m}$, where m equals 3 for very clean samples, 4 for strongly disordered samples, and 2 - 3 for samples of intermediate degree of disorder [19]. Since T_e is related to the applied voltage by $T_e \propto V^{2/(2+m)}$ [20], one obtains $\tau_{\varphi,ep} \propto V^{-2m/(2+m)}$ and $L_{\varphi,ep} \propto V^{-m/(2+m)}$. Our result $L_{\varphi}(V_{DC}) \propto V_{DC}^{-0.57 \pm 0.03}$ gives $m = 2.6 \pm 0.3$, which agrees well with the value of 2.5 obtained in a noise measurement on similar samples [21]. Moreover, our equilibrium WL result ($L_{\varphi,ep}(T) \propto T^{-m/2}$) is $m = 2.4$, in excellent agreement with the above values. Finally, we note that even though T_e rises up to $\sim 10 - 15$ K at high V_{DC} the energy averaging given by the LK approach remains essentially unaffected because T_e increases more slowly than the voltage itself.

In conclusion, we have measured the universal conductance fluctuations and Aharonov-Bohm effect in mesoscopic gold samples under highly non-equilibrium conditions of large applied bias voltages. The rms fluctuation δg_{rms} of the differential conductance increases with voltage $\propto \sqrt{V/V_c}$ as long as the inelastic scattering length is not much smaller than the sample length, which demonstrates the validity of the theoretical prediction by Larkin and Khmel’nitskiĭ. This increase is followed by a decay of δg_{rms} at higher voltages, where inelastic scattering becomes substantial. The decay is a power law for the universal conductance fluctuations and exponential in the case of the Aharonov-Bohm effect. The phase co-

herence length decreases with increasing bias voltage as $L_{\varphi}(V) \propto V^{-0.19 \pm 0.02}$ in the region of increasing $\delta g_{rms}(V)$ (region I) and as $L_{\varphi}(V) \propto V^{-0.57 \pm 0.03}$ when $\delta g_{rms}(V)$ decays (region II), which is in good agreement with the inferred $L_{\varphi}(V)$ dependences for (I) electron-electron and (II) electron-phonon scattering, respectively. In particular, dephasing by electron-electron collisions is not sufficient to suppress the enhancement mechanism. The decay of $\delta g_{rms}(V)$ occurs when phonons start to dominate dephasing. This work was supported by the Swiss National Science Foundation.

-
- [1] P. A. Lee and D. Stone, Phys. Rev. Lett. **55**, 1662 (1985).
 - [2] Y. Aharonov and D. Bohm, Phys. Rev. **115**, 485 (1959).
 - [3] A. I. Larkin and D. E. Khmel’nitskiĭ, Pis’ma Zh. Eksp. Teor. Fiz. **91**, 1815 (1986) [Sov. Phys. JETP **64** 1075 (1986)]; Phys. Scr. **T14**, 4 (1986).
 - [4] R. A. Webb, S. Washburn and C. P. Umbach, Phys. Rev. B **37**, 8455 (1988).
 - [5] S. B. Kaplan, Phys. Rev. B **38**, 7558 (1988).
 - [6] D. C. Ralph, K. S. Ralls and R. A. Buhrman, Phys. Rev. Lett. **70**, 986 (1993).
 - [7] R. Schäfer, K. Hecker, H. Hegger and W. Langheinreich, Phys. Rev. B **53**, 15964 (1996).
 - [8] C. Terrier, C. Strunk, T. Nussbaumer, D. Babić and C. Schönenberger, Fizika A (Zagreb) **8**, 157 (1999).
 - [9] R. Häussler, H. B. Weber and H. v. Löhneysen, J. Low Temp. Phys. **118**, 467 (2000).
 - [10] B. L. Al’tshuler and A. G. Aronov, Pis’ma Zh. Teor. Eksp. Teor. Fiz. **33**, 515 (1981) [JETP Lett. **33**, 499 (1981)].
 - [11] P. Mohanty, Physica B **280**, 446 (2000).
 - [12] A. B. Gougam, F. Pierre, H. Pothier, D. Esteve and N. O. Birge, J. Low Temp. Phys. **118**, 447 (2000).
 - [13] F. P. Milliken, S. Washburn, C. P. Umbach, R. B. Laibowitz and R. A. Webb, Phys. Rev. B **36**, 4465 (1987).
 - [14] Strictly speaking, the conditions are $V_{DC} \gg V_{c0}$ and $L_{\varphi} \ll L_{c0}$.
 - [15] D. P. DiVincenzo and C. L. Kane, Phys. Rev. B **38**, 3006 (1988).
 - [16] M. Henny, H. Birk, R. Huber, C. Strunk, A. Bachtold, M. Krüger and C. Schönenberger, Appl. Phys. Lett. **71**, 773 (1997), and references therein.
 - [17] M. Henny, S. Oberholzer, C. Strunk and C. Schönenberger, Phys. Rev. B **59**, 2871 (1999).
 - [18] H. Pothier, S. Gueron, Norman O. Birge, D. Est’eve, and M. H. Devoret, Phys. Rev. Lett. **79**, 3490 (1997).
 - [19] A. Schmid, in *Localization, Interaction and Transport Phenomena*, ed. by B. Kramer, G. Bergmann and Y. Bruynsereade, (Springer, Berlin, 1985).
 - [20] P. W. Anderson, E. Abrahams and T. V. Ramakrishnan, Phys. Rev. Lett. **43**, 718 (1979).
 - [21] M. Henny, PhD Thesis, University of Basel, 1998.